Lower Paleozoic 'El Nihuil Dolerites': Geochemical and Isotopic Constraints of Mafic Magmatism in an Extensional Setting of the San Rafael Block, Mendoza, Argentina

Carlos A. Cingolani, Eduardo Jorge Llambías, Farid Chemale Jr., Paulina Abre and Norberto Javier Uriz

Abstract The 'El Nihuil Mafic Unit' is exposed at the Loma Alta region northwards of the El Nihuil dam. This igneous body consists mainly of mafic rocks assigned to the Precambrian and Lower Paleozoic according to different authors. The mafic unit shows an elongated shape with a NNE–SSW orientation on the western side of the San Rafael Block (SRB), developed for a length of 17.5 km and with a maximum width of 4.2 km and is composed of deformed gabbros, amphibolites, and tonalites that represent the Mesoproterozoic continental crust, and dykes and sills of undeformed Lower Paleozoic porphyritic dolerites. We present the petrology, geochemistry, isotope data, and determinations of emplacement conditions of the dolerites that could represent a sliver of Cuyania-Chilenia terranes suture. The dolerites show classical porphyritic texture, with elongated subhedral plagioclase (andesine) and clinopyroxene phenocrysts. Geochemical analyses of El Nihuil Dolerite samples indicate that

C.A. Cingolani (✉) · E.J. Llambías
Centro de Investigaciones Geológicas, CONICET-UNLP,
Diag. 113 n. 275, CP1904 La Plata, Argentina
e-mail: carloscingolani@yahoo.com

E.J. Llambías
e-mail: llambias@cig.museo.unlp.edu.ar

F. Chemale Jr.
Programa de Pós-Graduação Em Geologia, Universidade Do Vale Do Rio Dos Sinos,
São Leopoldo, RS, Brazil
e-mail: faridcj@unisinos.br; faridchemale@gmail.com

P. Abre
Centro Universitario de la Región Este, Universidad de la República,
Ruta 8 Km 282, Treinta y Tres, Uruguay
e-mail: paulinabre@yahoo.com.ar

N.J. Uriz
División Geología, Museo de La Plata, UNLP,
Paseo Del Bosque s/n, B1900FWA La Plata, Argentina
e-mail: norjuz@gmail.com

C.A. Cingolani (ed.), *Pre-Carboniferous Evolution of the San Rafael Block, Argentina*, Springer Earth System Sciences,
DOI 10.1007/978-3-319-50153-6_6

the rocks are MORB-type basalts. In the P_2O_5 versus Zr diagram, the dolerites plot in the tholeiitic field similarly to western Cuyania basalts, and in the Th–Hf/3–Ta tectonic discrimination diagram the dolerite dykes plot mainly as E-MORB. Dolerite samples were dated by K–Ar (whole rock) systematic and the ages are 448.5 ± 10 and 434.2 ± 10 Ma (Upper Ordovician and close to the Lower Silurian boundary). The dolerites represent the unique Lower Paleozoic mafic rock outcrops within the SRB. $Nd_{(TDM)}$ ages are in between 0.51 and 0.80 Ga; $\varepsilon Nd_{(0)}$ record positive values ranging from +3.85 and +7.84; $\varepsilon Nd_{(t)}$ record +4.27 to +12.42. $^{87}Sr/^{86}Sr$ ratios are in between 0.7032 and 0.7050 in agreement with values for ocean ridge tholeiites. These mafic rocks are interpreted as a part of a dismembered 'Famatinian ophiolite belt' emplaced during the Lower Paleozoic extensional environment within a thinned Mesoproterozoic continental crust on western Cuyania terrane.

Keywords Lower Paleozoic · Extensional event · Mafic rocks · El Nihuil · Western Cuyania

1 Introduction

The pre-Andean region in west-central Mendoza province, Argentina, comprises the SSE-NNW Cenozoic structured San Rafael Block (SRB); towards East, it passes into the Pampean plains being covered by modern sedimentary and basaltic back-arc volcanic units. The northern and southern boundaries are limited by the Cuyo and Neuquén sedimentary basins, respectively. To the West, the Andean foothill bounds it (Fig. 1a). Paleontological and geological evidence allow interpreting the SRB as a southern extension of the Cuyania terrane (Ramos 2004). The Upper Paleozoic regional unconformity (Dessanti 1956) limits the so-called 'pre-Carboniferous units,' which includes diverse igneous-metamorphic and sedimentary units of Precambrian-Middle Paleozoic age. One of these igneous units, described and mapped as the intrusive 'gabbro' by Dessanti (1956) is exposed northwards of the El Nihuil dam (Fig. 1b). More recent studies (Cingolani et al. 2000, 2012) have demonstrated that the 'gabbro' is composed of mafic rocks of two different ages. The oldest rocks are Precambrian and consist of deformed gabbros, amphibolites, tonalites, whereas the youngest rocks are dolerites of Lower Paleozoic age. The dolerites record a NE–SW belt cropping out mainly in the Loma Alta sector (1434 m, 34°58′50″S and 68°45′00″W) and exposed at low hills within an overall smooth and rounded relief (Fig. 2).

This paper focuses in the Lower Paleozoic dolerites. Figure 1b shows the elongated shape of the mafic bodies on the western side of the SRB, developed for a length of 17.5 km and with a maximum width of 4.2 km. A southern extension is recorded on an isolated outcrop located to the south of the El Nihuil Lake (Fig. 1b).

The dolerites were studied using several techniques including geochemistry and geochronology in order to determine emplacement conditions; its importance relies in the fact that these rocks could represent a sliver of a terrane suture. Other lithological components of the mafic belt such as gabbros, amphibolites, and

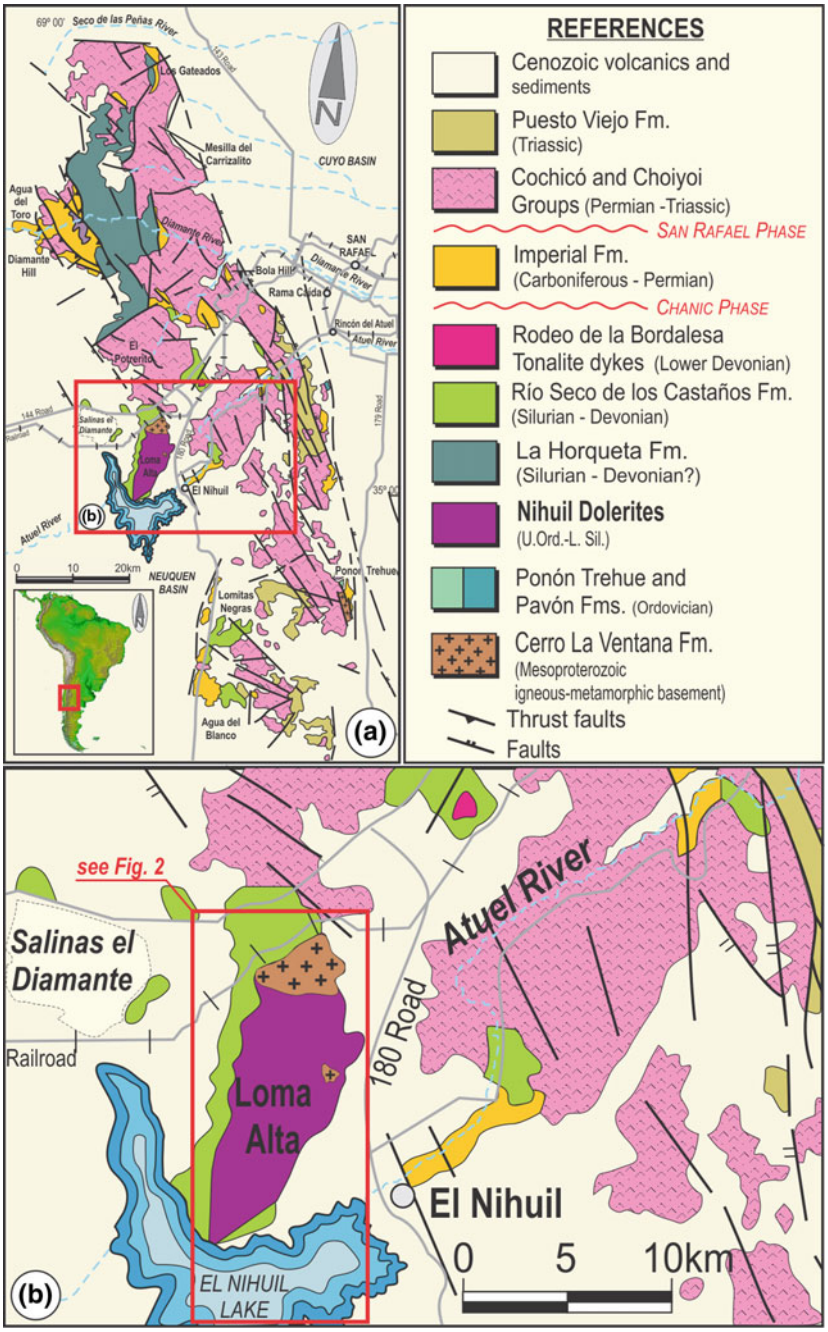

Fig. 1 **a** Geological sketch map of the San Rafael Block showing the location of the El Nihuil Dolerites and **b** details of the Lower Paleozoic dolerites exposed mainly in Loma Alta sector

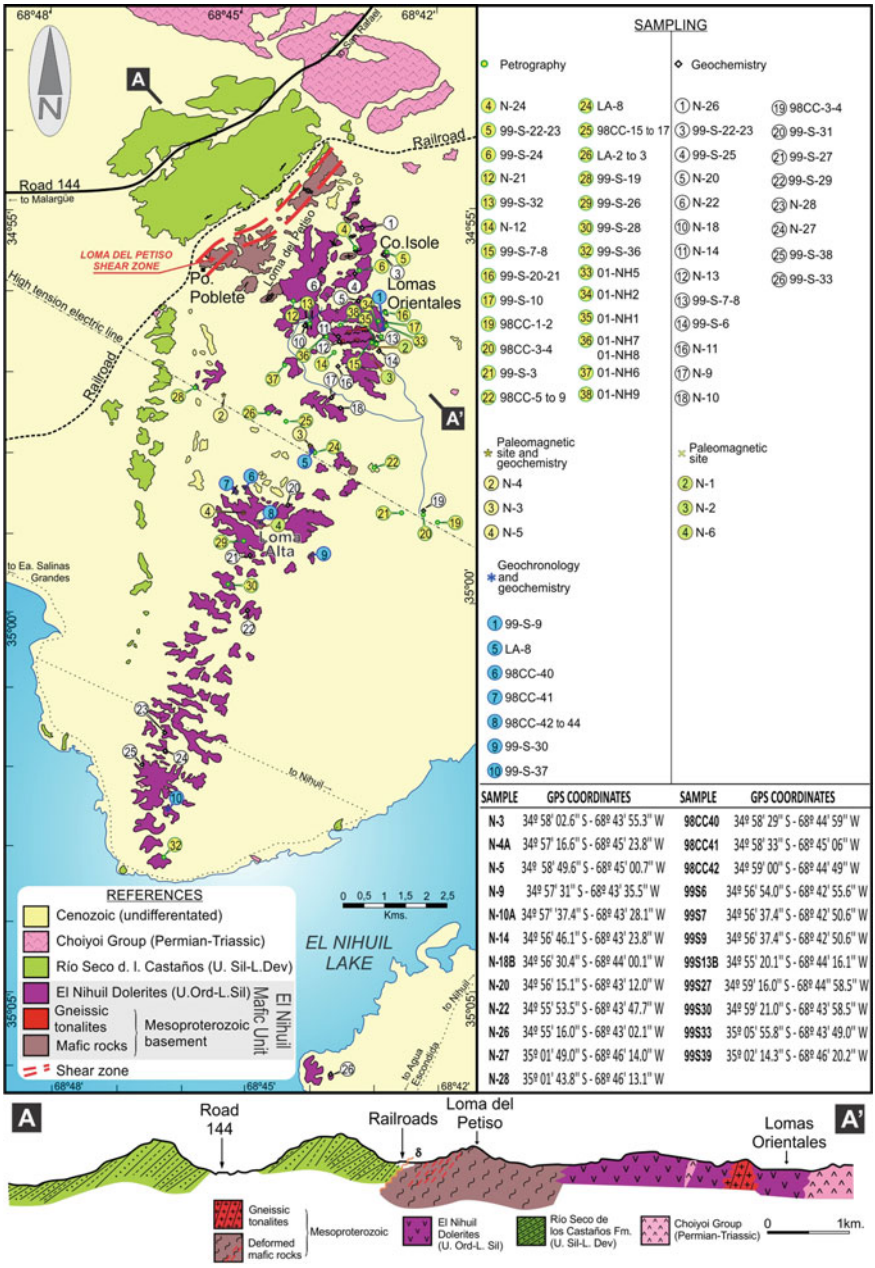

SAMPLE	GPS COORDINATES	SAMPLE	GPS COORDINATES
N-3	34º 58' 02.6" S - 68º 43' 55.3" W	98CC40	34º 58' 29" S - 68º 44' 59" W
N-4A	34º 57' 16.6" S - 68º 45' 23.8" W	98CC41	34º 58' 33" S - 68º 45' 06" W
N-5	34º 58' 49.6" S - 68º 45' 00.7" W	98CC42	34º 59' 00" S - 68º 44' 49" W
N-9	34º 57' 31" S - 68º 43' 35.5" W	99S6	34º 56' 54.0" S - 68º 42' 55.6" W
N-10A	34º 57' 37.4" S - 68º 43' 28.1" W	99S7	34º 56' 37.4" S - 68º 42' 50.6" W
N-14	34º 56' 46.1" S - 68º 43' 23.8" W	99S9	34º 56' 37.4" S - 68º 42' 50.6" W
N-18B	34º 56' 30.4" S - 68º 44' 00.1" W	99S13B	34º 55' 20.1" S - 68º 44' 16.1" W
N-20	34º 56' 15.1" S - 68º 43' 12.0" W	99S27	34º 59' 16.0" S - 68º 44" 58.5" W
N-22	34º 55' 53.5" S - 68º 43' 47.7" W	99S30	34º 59' 21.0" S - 68º 43' 58.5" W
N-26	34º 55' 16.0" S - 68º 43' 02.1" W	99S33	35º 05' 55.8" S - 68º 43' 49.0" W
N-27	35º 01' 49.0" S - 68º 46' 14.0" W	99S39	35º 02' 14.3" S - 68º 46' 20.2" W
N-28	35º 01' 43.8" S - 68º 46' 13.1" W		

Fig. 2 Geological sketch map of the 'El Nihuil Mafic Unit' based on Cingolani et al. (2000) and location of the dolerite samples obtained for different studies (petrography, geochemistry, isotope analyses and paleomagnetism). A–A′: NW–SE cross-section showing the contact relationships between the Lower Paleozoic dolerites and other units

tonalites with ductile deformation are described in the chapter about the Mesoproterozoic basement (Cingolani et al. this volume).

The present information still at reconnaissance level could be important to encourage more detailed works on these interesting mafic rocks of the SRB, which are important to unravel some aspects of the nature and history of tectonic terranes. It is known that the dolerite (diabase or microgabbro) is a mafic, holocrystalline, subvolcanic rock equivalent to volcanic basalt or plutonic gabbro. Dolerite dykes and sills are typically shallow intrusive bodies and often exhibit fine grained to aphanitic chilled margins and dark-colored rocks. The term 'diabase' is often used as a synonym of dolerite by American geologists, however, in Europe the term is usually only applied to altered dolerites. In ophiolitic complexes the dolerites are related with gabbros (base) and pillow lavas (top).

2 Previous Works

Mafic rocks within the SRB were first described during the geotechnical Atuel river studies by Wichmann (1928) and for the oil industry by Padula (1949). Later on, it was mapped as 'intrusive gabbro in the La Horqueta Serie' by Dessanti (1956) and assigned tentatively to the Precambrian. When Nuñez (1976) completed the field-base mapping, he described the mafic rocks as 'gabbros and porphyritic dolerites' cut by andesite dykes from the Choiyoi Group (Permian-Triassic). González Díaz (1981) mentioned gabbros with saussuritization processes intruded by lamprophyres and record the first Ordovician K–Ar ages.

Other authors (Criado Roqué and Ibañez 1979) described dolerite dykes interpreted as a part of a 'phacolit-type' igneous body with chilled margins. The first geochemical prospection work over the entire 'El Nihuil Mafic Unit' was presented by Davicino and Sabalúa (1990) they recognized porphyritic gabbros and dolerites, cataclastic rocks, mylonites and spilites and affected by two Tertiary faulted systems (N50–140° and N100–190°). Cingolani et al. (2000) reported more geochemical data along the mafic unit, that allows separating two different magmatic events: one composed of deformed gabbros, amphibolites, and tonalites; and the other of undeformed dolerites. More information about the regional geology of this sector of the SRB was presented by Sepúlveda (1999) and Sepúlveda et al. (2007).

3 Geological Aspects

'El Nihuil Mafic Unit' comprises two units: (i) Mesoproterozoic gabbros, amphibolites, and tonalites (Cerro La Ventana Fm.) developed mainly at the 'Loma del Petiso shear zone' and Lomas Orientales, (ii) Upper Ordovician-Lower Silurian undeformed porphyritic dolerites (Fig. 2) developed along the central and southern sector of the body (Cingolani et al. 2000). Similar structural style and

Mesoproterozoic isotopic ages obtained from isolated deformed tonalite rocks (equivalents to deformed gabbros mentioned before) from Lomas Orientales as recorded by Cingolani et al. (2012) suggest that all deformed rocks with overprinted ductile deformation correspond to the Mesoproterozoic continental crust relicts.

Furthermore, deformed mafic rocks outcropping at the 'Loma del Petiso shear zone' in unconformity with the Río Seco de los Castaños Fm (Silurian-Devonian), display cross-cutting relationships supporting that the dolerite dykes were afterwards intruded (Fig. 3a, b). The sedimentary Upper Ordovician (Pavón Fm) that was the most probably country rocks of the dolerites were not recorded along the 'El Nihuil Mafic Unit.' The Pavón Fm records detrital chromian spinels derived from mid-ocean ridge and continental flood basalts. The El Nihuil Mafic Unit was considered as a probable source of these spinels (Abre et al. 2009), and although the dolerites were emplaced in the same tectonic setting as the source rocks of the spinels, such a derivation is not supported by isotopic ages, because dolerites are younger than the Pavón Fm. Detrital zircon ages from Pavón Fm confirmed a main Mesoproterozoic source (Abre et al. this volume), therefore a provenance of chromian spinels from the Mesoproterozoic section of the El Nihuil mafic body cannot be yet ruled out.

In summary, it is clear that the exposed country rocks of the Lower Paleozoic undeformed extrusive dolerites are only the deformed gabbro, amphibolites, and

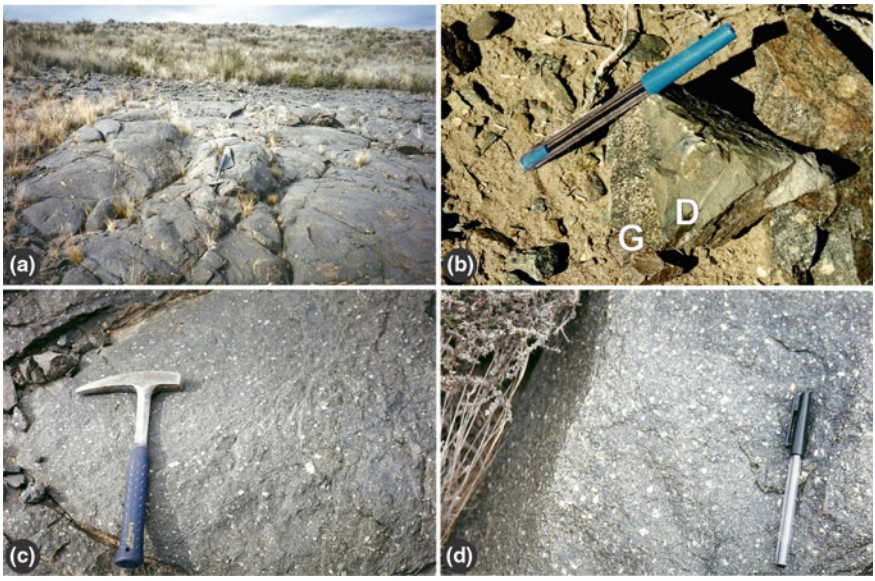

Fig. 3 **a** A general view of the dolerite outcrops taken towards the North, near Loma Alta region in the 'El Nihuil Mafic Unit,' **b** details of the dolerite (D) that is intrusive in the deformed gabbros (G), **c** and **d** both pictures showing the typical texture of the dolerites with plagioclase and clynopiroxene phenocrysts

tonalite type rocks interpreted as part of the Mesoproterozoic basement (Cerro La Ventana Formation; Cingolani et al. this volume).

4 Petrology and Geochemistry

In hand specimen the color of undeformed porphyritic dolerites is dark, medium or dark-gray, or greenish (Fig. 3a). The porphyritic texture is clearly observed in several outcrops with fine and centimeter white/pale phenocrysts (Fig. 3c, d).

The dolerites show classical porphyritic texture (Fig. 4), with elongated subhedral plagioclase (andesine) and clinopyroxenes phenocrysts; the finer matrix has a subophitic texture and it is composed of anhedral plagioclase enclosing clinopyroxenes or amphiboles. Hornblende and tremolite-actinolite amphiboles are commonly replacing pyroxenes. Accessory minerals are apatite, opaque minerals and finely disseminated pyrite. Olivine crystals were also recognized in some samples.

Fifteen dolerite whole rock samples were selected to be analysed for major, minor, and trace elements (including REE) at ACTLABS, Canada; using a lithium metaborate/tetraborate fusion procedure with measurements done by ICP-MS; results are shown on Table 1. SiO_2 concentrations varying from 46.07 to 49.34% and $Na_2O + K_2O$ contents less than 4 wt% allow classifying the dolerites as basalts (Le Maitre 1989). MgO concentrations vary between 5.88 and 7.77%, while FeO ranges from 6.92 to 8.94%. Alkalis show low concentrations, ranging from 0.25 to 0.77% for K_2O and between 2.11 and 3.37% for Na_2O; wt% TiO_2 is relatively high (1.12–2.19%) and wt% MnO and P_2O_5 values are less than 0.29%; Na_2O concentration have an average of 2.58 wt%, that could indicate absence of albitization processes. Loss on ignition (LOI) is in between 1.09 and 4.5% indicating moderate to high alteration. Cr = 207, Sc = 45, and Ni = 101 ppm averages indicate moderate concentrations (Table 1).

To classify the dolerite rocks we employed diagrams based in immobile elements. According to the Zr/TiO_2 versus Nb/Y rock classification diagram (Winchester and Floyd 1977) the El Nihuil Dolerite samples plotted in the field of andesite/basalts (Fig. 5a), although according to their maximum SiO_2 content (anhydrous base) of 51.5% they are recorded as basalts. The distribution of major oxides indicates the effects of secondary processes (weathering), but despite this the samples have the chemical characteristics of the tholeiitic series, as shown in the AFM diagram (Irvine and Baragar 1971; Fig. 5b). Following Pearce and Cann (1973), the Ti/100 – Zr − Y/3 and Ti/100 – Zr − Sr/2 diagrams indicate that the dolerites correspond to MORB-type rocks (Fig. 6a, b). La/Yb normalized ratios between 0.93 and 1.44 (Table 2) fall within the range of values occurring in mid-ocean ridge volcanic rocks (Gale et al. 2013). The Th/U ratios between 3.53 and 4.56 are close to E-MORB and Zr/Y ratios ranging from 2.15 to 2.86 suggest continental crust contamination (Arévalo and McDonough 2010).

In the P_2O_5 versus Zr diagram (Fig. 7a) for basalts classification after Winchester and Floyd (1976), the El Nihuil Dolerite samples plot in the tholeiitic

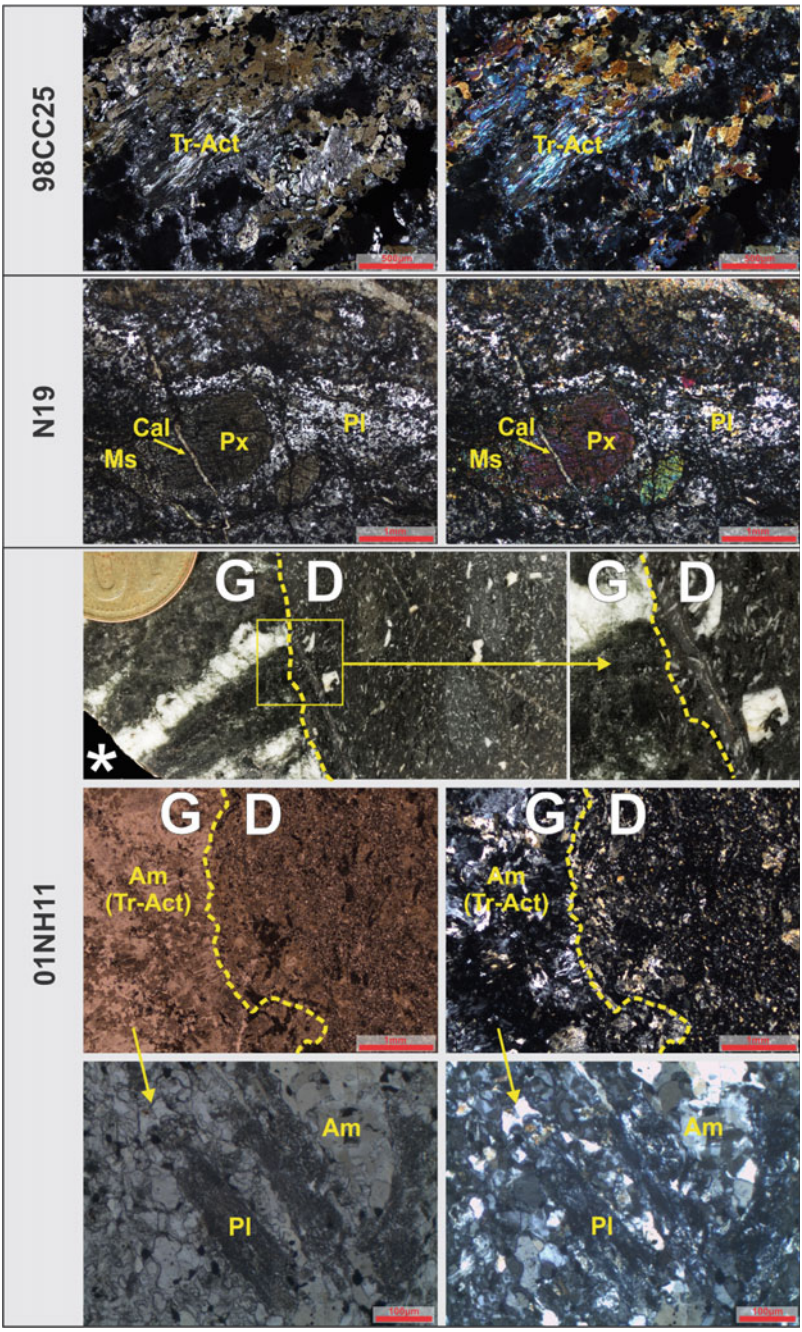
98CC25
Tr-Act
Tr-Act
N19
Cal
Ms
Px
Pl
Cal
Ms
Px
Pl
01NH11
G D
G D
*
G D
Am
(Tr-Act)
G D
Am
(Tr-Act)
Am
Pl
Am
Pl

◂**Fig. 4** Photomicrographs of dolerite samples (98CC25, N19 and 01NH11) showing the texture and main mineralogical composition. On the *left*, //nicols; on the *right* X nicols. Sample 01NH11 records the intrusive contact between dolerite (D) and gabbro (G) like rocks. *Tr-Act* tremolite-actinolite; *Pl* plagioclase; *Am* amphibole; *Px* Pyroxene; *Ms* muscovite; *Cal* calcite. * shown gabbro-dolerite contact in the polished hand specimen. The coin as scale is 1.5 cm

field close to the western Cuyanian basalts (Boedo et al. 2013). As shown in Fig. 7b, the Th–Hf/3–Ta tectonic diagram (Wood et al. 1979), that can discriminate silicic magmas derived from E-type MORB or WPB and those associated with destructive plate margins or remelted continental crust) the dolerite dykes are plotted mainly in E-MORB field (intraplate oceanic basalts). Basaltic dykes, sills, and flows from Precordillera mafic-ultramafic belt after Boedo et al. (2013) are also plotted for comparison (green-shaded field).

In Fig. 8a the primordial mantle normalized trace elements show enrichment in Cs, Rb, Ba, and Nb compared to the average pattern of N-MORB. Chondrite-normalized REE diagrams (Fig. 8b) show El Nihuil dolerite patterns parallel to average N-MORB, but enrichments of the lighter elements (LREE) are evident, particularly for La and Ce. The La_n/Lu_n ratio is between 0.99 and 1.48. The normalized ratios data presented in Table 2 are similar to those from the Precordilleran basalts (Ramos et al. 2000; Boedo et al. 2013).

From the comparison to the N-MORB pattern, an enrichment of LIL (large ion lithophile) elements is evident, whereas the HFSE (high field strength elements) does not show such behavior. LIL elements could be enriched due to alteration of the rock or contamination with crustal material.

5 Isotopic Data

5.1 K–Ar

First K–Ar whole rock data was presented by González Díaz (1981), and indicate ages of 474 and 484 Ma for the "gabbro Loma Alta," however precision on sample locations was lacking (Linares et al. 1987). Two new fresh samples from El Nihuil Dolerites were dated by K–Ar whole rock systematic at the Centro de Pesquisas Geocronológicas, Universidade de São Paulo (Brazil). As we can see in the Table 3 the obtained ages are 448.5 ± 10 and 434.2 ± 10 Ma, dating the extrusive event as Upper Ordovician and close to the Lower Silurian boundary. Such age determination undoubtedly confirmed that the dolerites represent the unique Lower Paleozoic mafic belt within the SRB.

Table 1 Geochemical data (ACTLABS, Canada) of major, minor, and trace elements (including REE) of the studied dolerite rocks. Negative values mean below detection limits

SAMPLE	SiO_2 %	Al_2O_3 %	Fe_2O_3 %	ox calc.	FeO calc.	Fe_2O_3 calc.	MnO %	MgO %	CaO %	Na_2O %	K_2O %	TiO_2 %	P_2O_5 %	LOI %	TOTAL %	Sr ppm	K ppm	Cs ppm	Rb ppm	Ba ppm	Th ppm	U ppm	Ta ppm	Nb ppm	Zr ppm
N-3	48.77	14.23	13.68	0.66	8.46	4.28	0.214	6.47	10.96	2.37	0.42	1.802	0.19	1.21	100.32	149	0.35	0.9	12	127	0.42	0.11	0.6	8.7	114
N-4A	46.07	13.65	14.13	0.66	8.63	4.54	0.196	7.25	7.47	3.37	0.33	1.433	0.15	4.53	98.58	129	0.27	0.5	4	268	0.28	0.07	0.3	4.6	79
N-5	49.00	14.38	11.97	0.67	7.42	3.73	0.205	6.92	11.37	2.39	0.28	1.553	0.17	1.13	99.36	135	0.23	1.0	8	95	0.34	0.10	0.5	5.5	97
N-9	47.90	15.38	11.44	0.66	7.04	3.62	0.181	7.22	10.72	2.35	0.77	1.416	0.16	2.15	99.67	182	0.64	0.6	20	266	0.33	0.09	0.4	4.9	81
N-10A	48.47	13.93	13.42	0.67	8.33	4.16	0.225	6.84	11.11	2.44	0.25	1.824	0.21	1.77	100.50	179	0.21	0.3	6	135	0.45	0.13	0.6	5.8	91
N-14	47.62	15.62	11.79	0.67	7.37	3.60	0.193	6.04	11.55	2.11	0.54	1.514	0.18	2.60	99.75	234	0.45	1.1	15	220	0.42	0.12	0.6	5.9	87
N-18	48.38	13.55	13.71	0.67	8.50	4.26	0.218	6.57	10.48	2.20	0.57	1.963	0.23	1.25	99.12	149	0.47	2.0	15	234	0.48	0.13	0.7	6.7	116
N-20	47.51	14.96	11.18	0.67	6.97	3.43	0.185	7.77	10.83	2.33	0.41	1.349	0.16	2.54	99.21	197	0.34	0.4	10	229	0.38	0.10	0.6	4.6	72
N-22	47.65	13.79	14.57	0.66	8.94	4.64	0.227	5.88	9.19	3.00	0.25	2.169	0.29	2.45	99.47	144	0.21	0.7	6	107	0.69	0.18	0.7	9.2	138
N-26	47.64	15.61	11.71	0.67	7.30	3.60	0.187	6.12	11.32	2.28	0.46	1.482	0.16	3.03	99.99	212	0.38	1.3	12	186	0.35	0.10	0.6	4.6	82
N-27	49.34	14.92	11.14	0.67	6.92	3.45	0.172	7.59	12.01	2.12	0.39	1.209	0.11	1.16	100.17	126	0.32	0.5	10	140	0.28	0.08	0.5	2.7	55
N-28	48.93	14.87	11.60	0.67	7.22	3.58	0.184	7.17	11.98	2.24	0.31	1.387	0.14	1.09	99.90	158	0.26	1.2	9	126	0.30	0.08	1.0	3.6	66
98CC42	48.7	13.92	12.28				0.19	6.71	11.34	2.63	0.35	1.62	0.17	1.21	99.1	158		0.5	9.4	138	0.41	0.09	0.55	5.4	95
98CC40	47.76	15.21	11.77				0.19	6.43	10.67	2.7	0.7	1.48	0.14	2.17	99.22	179		1.5	17	159	0.45	0.1	0.57	4.7	83
98CC41	48.15	16.11	10.8				0.17	6.9	11.95	2.44	0.28	1.12	0.11	1.88	99.92	153		1	6.1	84	0.26	0.06	0.56	3.2	52

SAMPLE	Hf ppm	Ti ppm	Y ppm	V ppm	Cr ppm	Co ppm	Ni ppm	Cu ppm	Zn ppm	Ga ppm	Tl ppm	Pb ppm	La ppm	Ce ppm	Pr ppm	Nd ppm	Sm ppm	Eu ppm	Gd ppm	Tb ppm	Dy ppm	Ho ppm	Er ppm	Tm ppm	Yb ppm	Lu ppm
N-3	3.1	6.576	40.4	395	195	49	321	114	71	19	0.10	-5	5.92	15.1	2.33	12.5	3.99	1.50	5.24	1.05	6.74	1.40	4.03	0.603	3.94	0.595
N-4A	2.3	4.482	31.8	279	152	19	69	241	-30	11	-0.05	-5	4.58	11.8	1.82	9.85	3.23	1.00	4.41	0.85	5.46	1.19	3.33	0.497	3.12	0.474
N-5	2.9	6.822	37.6	346	216	41	109	89	46	18	-0.05	-5	5.59	14.5	2.20	11.9	3.92	1.49	5.23	1.02	6.60	1.36	3.92	0.610	3.76	0.585
N-9	2.5	6.432	30.7	302	255	45	118	98	61	17	0.42	5	5.37	13.5	2.01	10.8	3.38	1.32	4.53	0.85	5.46	1.14	3.14	0.490	3.06	0.469
N-10A	2.8	6.666	39.0	371	184	29	106	64	-30	16	-0.05	-5	6.92	17.0	2.49	13.1	4.09	1.57	5.43	1.04	6.67	1.39	3.95	0.580	3.81	0.565
N-14	2.5	6.93	32.7	315	184	18	97	51	-30	15	-0.05	-5	6.62	15.9	2.31	11.9	3.68	1.42	4.74	0.90	5.48	1.15	3.28	0.492	3.12	0.470
N-18	3.5	6.288	44.4	396	181	47	141	76	101	19	0.15	-5	7.38	18.5	2.77	14.7	4.45	1.68	5.99	1.15	7.36	1.56	4.45	0.680	4.13	0.656
N-20	2.2	6.498	29.6	290	285	43	138	83	36	16	0.06	-5	5.21	12.6	1.86	9.98	3.18	1.22	4.17	0.77	4.96	1.06	2.95	0.437	2.78	0.419
N-22	4.2	5.514	48.4	389	128	46	116	66	93	19	0.08	-5	9.62	23.8	3.44	18.2	5.39	1.82	7.09	1.30	8.37	1.76	4.98	0.752	4.69	0.716
N-26	2.5	6.792	33.2	334	203	45	123	95	85	18	0.09	-5	5.13	13.0	1.95	10.7	3.52	1.33	4.54	0.89	5.68	1.22	3.44	0.522	3.25	0.503
N-27	1.8	7.206	25.8	256	218	15	75	22	-30	11	-0.05	-5	3.62	9.0	1.41	7.60	2.53	1.01	3.44	0.67	4.28	0.94	2.66	0.401	2.62	0.384
N-28	2.1	7.188	28.8	280	164	17	70	12	-30	12	-0.05	-5	4.77	11.6	1.72	9.32	2.98	1.13	3.95	0.77	4.92	1.07	3.05	0.457	2.79	0.434
98CC42	2.8		35	345	403	49	63	49	57	18	-0.1		5.87	14.6	2.194	11.6	3.92	1.4	5.38	0.98	6.16	1.32	4.08	0.602	3.79	0.58
98CC40	2.5		29	316	377	47	51	99	72	19	0.1		4.89	12.6	1.877	10.1	3.35	1.241	4.8	0.82	5.18	1.11	3.44	0.511	3.15	0.496
98CC41	1.7		24	282	384	36	55	81	29	14	-0.1		3.78	9.4	1.392	7.22	2.53	1.01	3.64	0.64	4.03	0.89	2.71	0.398	2.49	0.398

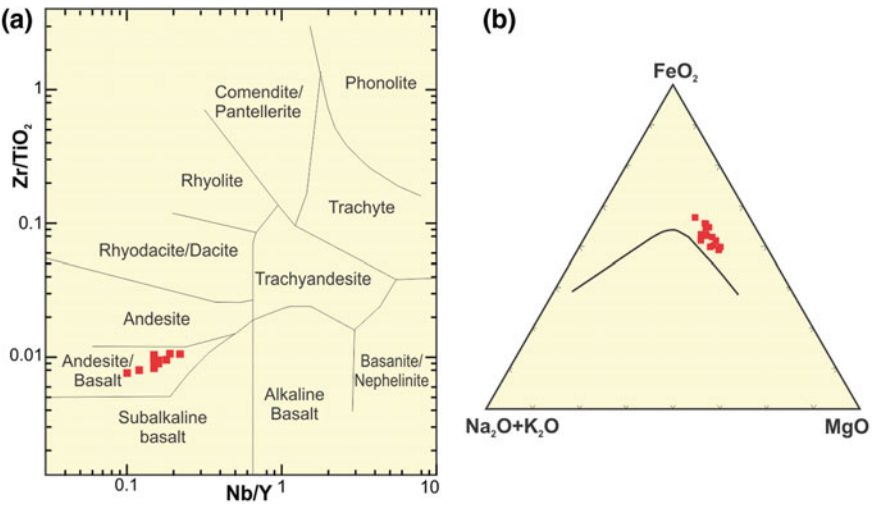

Fig. 5 **a** Classification diagram after Winchester and Floyd (1977) and **b** AFM diagram showing that samples belong to the tholeiitic series (Irvine and Baragar 1971)

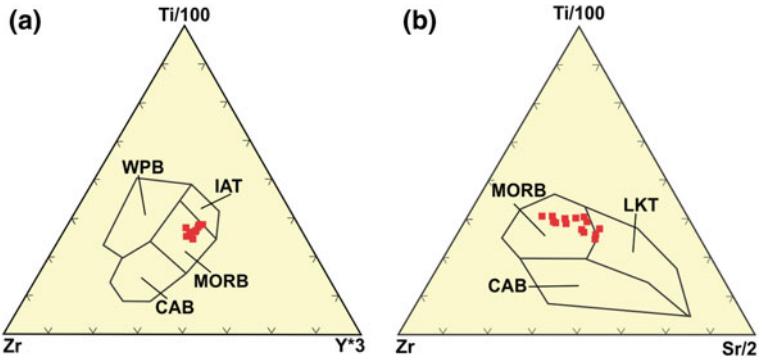

Fig. 6 In both tectonic discrimination diagrams **a** Ti/100 – Zr − (Y + 3) (after Pearce and Cann 1973) and **b** Ti/100 – Zr − Sr/2, dolerite rocks plot within the field of MORB (mid-ocean-ridge basalt). *WPB* within-plate basalt, *CAB* calc-alkaline basalt, *IAT* island arc tholeiites, *LKT* low-K tholeiites

5.2 Sm–Nd

Ten whole rock dolerite samples were used for Sm–Nd isotopic analyses (Table 4). The isotope dilution technique for Sm–Nd (using combining ^{149}Sm–^{150}Nd spike during August 2000) as well as the mass spectrometry for Sm and Nd, were carried out at the Laboratorio de Geología Isotópica, Universidade Federal do Río Grande do Sul, Porto Alegre (Brazil). The isotopic ratios were measured using the VG354

Table 2 Geochemical selected ratios of dolerite samples (n): normalized to chondrite after Taylor and McLennan (1985)

Samples	La/Yb (n)	La/Sm (n)	Sm/Yb (n)	La/Ta	Th/U	Zr/Y
N-3	1.02	0.94	1,09	9.60	3.90	2.82
N-4A	0.99	0.89	1.11	14.67	4.10	2.48
N-5	1.00	0.90	1 12	10.47	3.53	2.59
N-9	1.18	1.00	1.19	12.53	3.75	2.64
N-10A	1.23	1.06	1.15	11.76	3.54	2.32
N-14	1.44	1.13	1.27	11.52	3.55	2.66
N-1B	1.21	1.05	1.16	10.08	3.74	2.63
N-20	1.27	1.03	1.23	9.23	3.73	2.44
N-22	1.39	1.12	1.24	13.21	3.88	2.86
N-27	0.93	0.90	1.03	7.03	3.77	2.15
N-28	1.16	1.01	1.15	4.89	3.88	2.30
98CC42	1.05	0.94	1.11	10.67	4.56	2.71
98CC40	1.05	0.92	1,14	8.58	4.50	2.86
98CC41	1.03	0.94	1.09	6.75	4.33	2.17

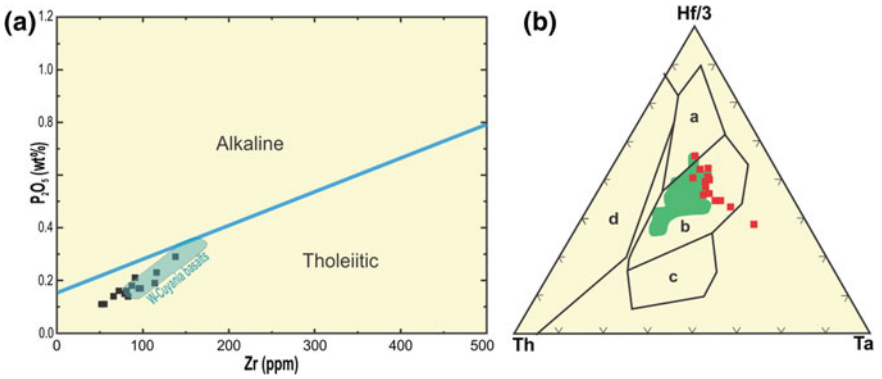

Fig. 7 **a** Classification diagram after Winchester and Floyd (1976). *Squares* in *black* are the El Nihuil Dolerites. For comparison the field of Western Cuyania basalts is shown (Boedo et al. 2013) and **b** tectonic discrimination diagram after (Wood et al. 1979). *Red squares* are the El Nihuil Dolerite samples. Fields *a* N-MORB; *b* E-MORB; *c* WPB; *d* VAB. Samples studied by Boedo et al. (2013) are shown for comparison as a *green-shaded area*

mass spectrometer with multiple collector system. The Nd model ages were calculated using single stage after DePaolo (1981) and second stage after Liew and Hofmann (1988) (Table 4). Epsilon Nd $_{(0)}$ values for the samples are in between +3.85 and +7.84 while $\varepsilon Nd_{(t = 450\ Ma)}$ record positive values (Fig. 9) ranging from +4.27 to +12.42. Nd model ages (two stage depleted mantle) are in between 0.51 and 0.80 Ga. These values are very close due to fractionation of Sm–Nd from −0.01 to −0.03 (Table 4). Sample N4-A has a higher $\varepsilon Nd_{(t = 450\ Ma)}$ value and a

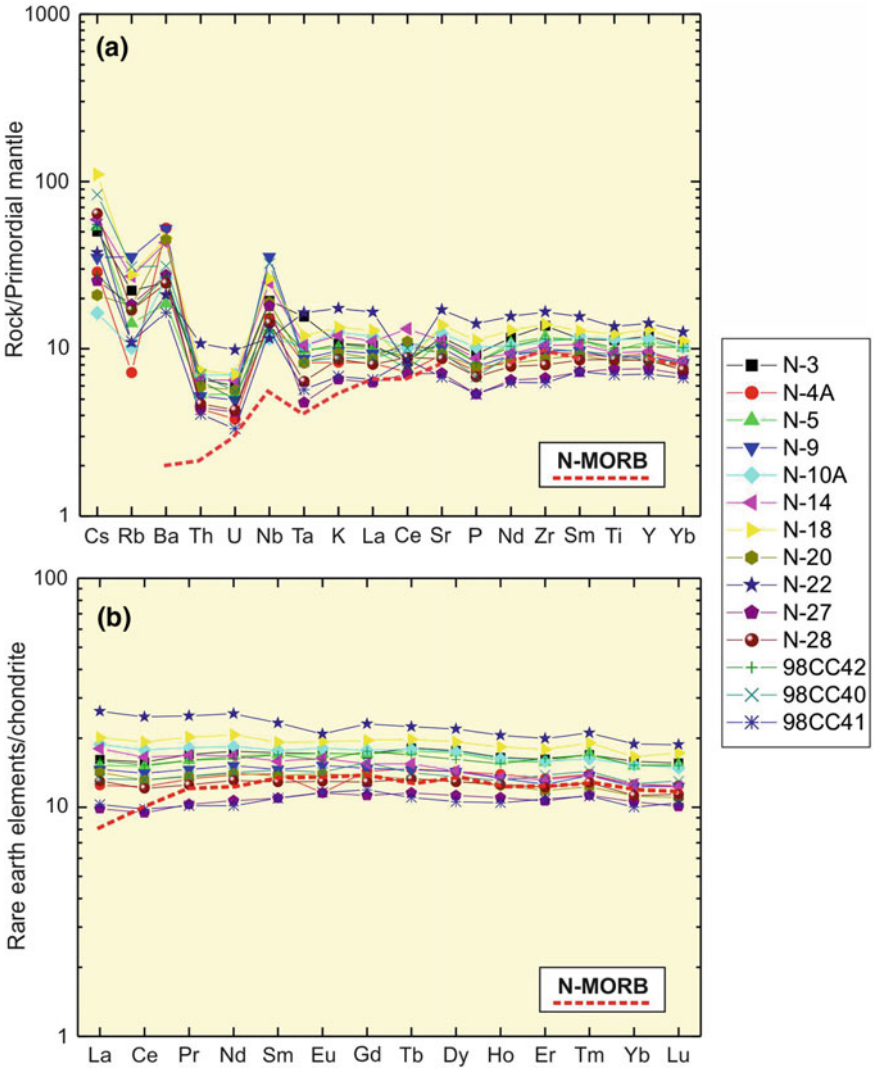

Fig. 8 **a** Primordial mantle normalized trace element diagram obtained from El Nihuil Dolerite samples and **b** chondrite-normalized REE diagram (Taylor and McLennan 1985). In both diagrams N-MORB average pattern is shown in *red*

Table 3 K–Ar laboratory (CPGeo, USP, Brazil) data for two dolerite samples

K–Ar EL Nihuil Dolerites									
SPK	Field No.	Material	Rock type	K%	Error	Ar40Rad ccSTP/g	Ar40 ATM	Age Ma	Error Ma
7729	99S9 A60	Whole rock	Dolerite	0.4017	0.6667	7.944	11.23	448.5	10
7730	99S30 A60	Whole rock	Dolerite	0.3095	0.5	5.901	15.23	434.2	10

Table 4 Sm–Nd whole rock data

Sample	Sm (ppm)	Nd (ppm)	$^{147}Sm/^{144}Nd$	$^{143}Nd/^{144}Nd$	±2s	*e*Nd (0)*	*e*Nd (*t*)**	*f*Sm–Nd	T_{DM} (Ga)***	$T_{DM\ 2.Stage}$ (Ga)****
N4-A	1.7	10.1	0.099	0.512987	20	6.81	12.42	−0.49	0.22	
N5	3.8	11.8	0.193	0.513006	24	7.17	7.37	−0.02	0.86	0.55
N27	2.6	7.7	0.202	0.513001	24	7.07	6.77	0.03	1.35	0.60
N28	3.1	9.5	0.194	0.513040	19	7.84	8.02	−0.02	0.67	0.51
99S29	3.1	9.2	0.203	0.513012	59	7.29	6.96	0.03	1.29	0.59
99S33	2.8	8.9	0.189	0.512835	41	3.85	4.27	−0.04	1.62	0.80
99S6	2.6	8.4	0.189	0.512922	41	5.53	5.98	−0.04	1.17	0.67
99S27	2.1	6.3	0.200	0.512968	55	6.43	6.24	0.02	1.49	0.65
N9	2.7	8.5	0.190	0.512954	48	6.17	6.53	−0.03	1.05	0.62
99S30	4.2	12.7	0.198	0.512875	14	4.62	4.56	0.01	1.99	0.78

Mean of 100 isotope ratios with ionic intensity of 1.0V for ^{146}Nd and multicollector with ^{146}Nd axial collector

*Calculated assuming $^{143}Nd/^{144}Nd$ today = 0.512638 with data normalized to $^{146}Nd/^{144}Nd$ = 0.72190. Epsilon Nd(0) = (($^{143}Nd/^{144}Nd$[sample, now]/0.512638) − 1) × 10^4

**eNd(t) = (($^{143}Nd/^{144}Nd$[sample, t]/143Nd/144Nd[CHUR, t]) − 1) × 10^4. t = crystallization age based on Ar–Ar WR age

***Calculated following model of DePaolo (1981)

****Two stage depleted mantle Nd model age calculated after Liew and Hofmann (1988)

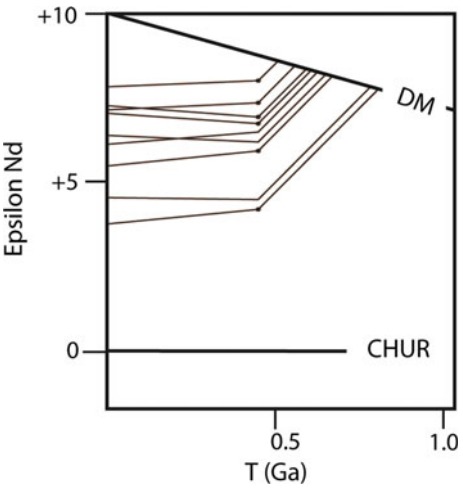

Fig. 9 εNd diagram showing second stage T_{DM} ages and positive εNd values for t = 450 Ma (see text for explanation)

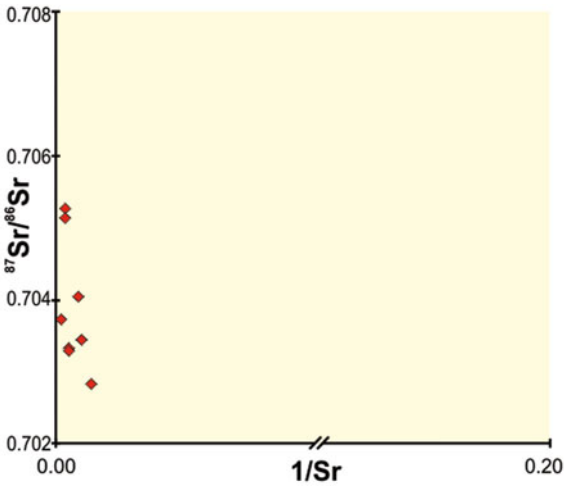

Fig. 10 Plot of samples in the $^{87}Sr/^{86}Sr$ versus 1/Sr diagram

$Nd_{T_{DM}}$ age younger than the crystallization age, but the f_{Sm-Nd} is indicating that these aberrant values are consequence of REE remobilization, probably due to alteration as deduced by LILE enrichments.

5.3 $^{87}Sr/^{86}Sr$ Ratios

The $^{87}Sr/^{86}Sr$ isotopic ratios were applied using eight whole rock dolerite samples obtained along the central and southern region of the 'El Nihuil Mafic Unit'

Table 5 Rb–Sr laboratory data

LAB no.	Sample no.	Rb (ppm)	Sr (ppm)	1/Sr	$^{87}Sr/^{86}Sr$ (Y)	$^{87}Rb/^{86}Sr$ (X)	T (Ma) $\lambda = 1.42$	$(^{87}Sr/^{86}Sr)_0$ T (Ma)
CIG 1103	N9	23.4	200.9	0.0049776	0.70643	0.337	450	0.70427
CIG 1106	99S27	24.8	176.7	0.0056593	0.70633	0.406	450	0.70372
CIG 1195	99S7	7.6	190.5	0.0052493	0.70458	0.116	450	0.70384
CIG 1196	99S13B	6.8	342.6	0.0029189	0.70369	0.057	450	0.70332
CIG 1198	99S30	20.6	168.6	0.0059312	0.70566	0.354	450	0.7034
CIG 1199	99S39	8.7	129.3	0.007734	0.7042	0.195	450	0.70295
CIG 1200	N3	13.1	151.5	0.0066007	0.70433	0.25	450	0.70323
CIG 1202	N27	12.6	135.9	0.0073584	0.70509	0.268	450	0.70509

(Fig. 2). The sample preparation and extraction of natural Sr through cation exchange columns was performed at the Centro de Investigaciones Geológicas, Universidad Nacional de La Plata, Argentina and mass-spectrometer analyses were performed at the Centro de Pesquisas Geocronológicas, University of São Paulo, Brazil. As it is shown in Fig. 10 and Table 5 the $^{87}Sr/^{86}Sr$ ratios are in between 0.7032 and 0.7050 in agreement with ocean ridge tholeiites.

6 The Western Precordillera Mafic Belt: A Comparison

Haller and Ramos (1984), Ramos et al. (1999) and Ramos (2004) were the authors that linked the mafic-type rocks and their extension to the tectonic suture zone between Chilenia and Cuyania terranes in the proto-Andean margin of Gondwana (Fig. 11). However, the ophiolitic signature of the mafic and ultramafic belt developed along western Precordillera was established by Borrello (1963, 1969). This mafic belt that extends over ca. 1000 km from south to north was named by Haller and Ramos (1984, 1993) as the 'Famatinian ophiolites' emplaced as a disrupted ophiolite during the Early Paleozoic (Ramos et al. 1984, 1986) Mahlburg Kay et al. (1984) based on geochemical data proposed that the western Precordillera mafic rocks could have formed in a broad back-arc basin or at a mid-ocean ridge with an enriched source or as an early oceanic rift next to a continental margin. Davis et al. (1999) challenged this interpretation suggesting the occurrence of two different sections of an ophiolite assemblage in Western Precordillera a Proterozoic one and another of Early Paleozoic age. More recently Boedo et al. (2013) discussed the E-MORB (enriched-type MORB) like signature of the mafic dykes and sills studied along the western Precordillera mafic-ultramafic belt as part of a non-subduction related ophiolite. González Menéndez et al. (2013) argued that the studied mafic rocks related to subduction or either N-MORB or OIB environment derived from primordial garnet-spinel transition mantle sources. The model supports a thinned continental margin between Chilenia and Cuyania terranes

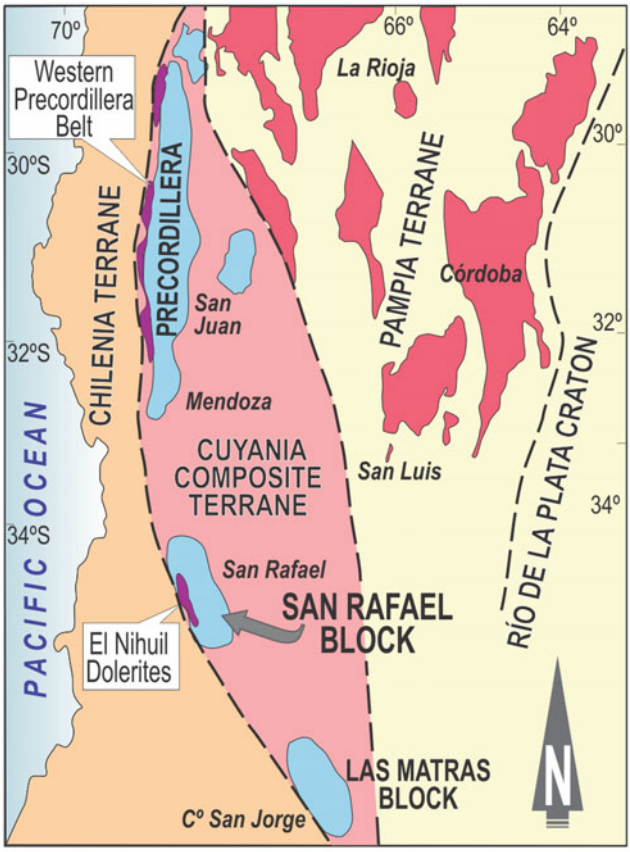
70º
66º
64º
30º
32º
34º
30ºS
32ºS
34ºS
Western Precordillera Belt
PRECORDILLERA
CHILENIA TERRANE
PACIFIC OCEAN
La Rioja
PAMPIA TERRANE
Córdoba
San Juan
Mendoza
CUYANIA COMPOSITE TERRANE
San Luis
RÍO DE LA PLATA CRATON
San Rafael
SAN RAFAEL BLOCK
El Nihuil Dolerites
LAS MATRAS BLOCK
Cº San Jorge
N

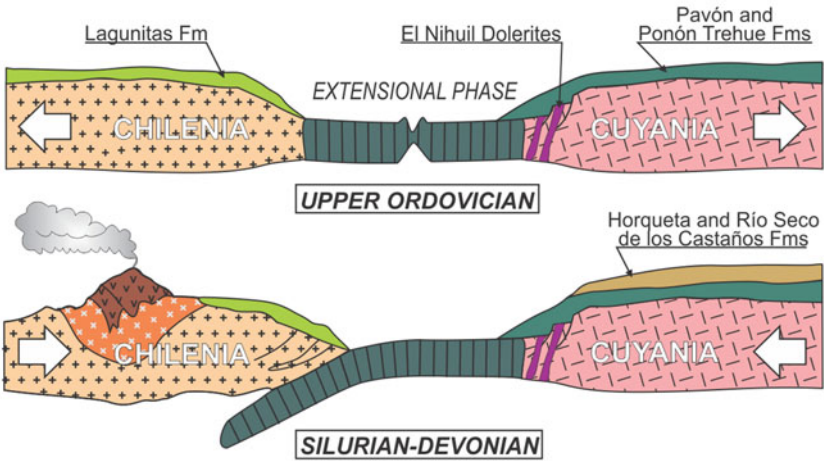
Lagunitas Fm
El Nihuil Dolerites
Pavón and Ponón Trehue Fms
EXTENSIONAL PHASE
CHILENIA
CUYANIA
UPPER ORDOVICIAN
Horqueta and Río Seco de los Castaños Fms
CHILENIA
CUYANIA
SILURIAN-DEVONIAN

◂**Fig. 11** **a** Location of the western Precordillera mafic belt in the context of the Cuyania terrane, **b** tectonic diagram showing the *Lower* Paleozoic extensional phase and intrusion of the El Nihuil Dolerites in a western continental margin of Cuyania. Ordovician sedimentary sequences are exposed over Cuyania (Ponón Trehué and Pavón Fms) and Lagunitas Fm in the eastern border of Chilenia terrane, and **c** during Silurian-Devonian time, west vergence subduction is developed generated a magmatic arc in Chilenia terrane before terranes collision during the Chanic tectonic phase

('Occidentalia terrane' after Dalla Salda et al. 1998) during the Middle to Late Ordovician. Many authors (Alonso et al. 2008 and references therein) described an extensional regime developing in a passive margin environment during the Ordovician in the western margin of Precordillera. These data were discussed in several geotectonic models proposed by different authors such as Ramos et al. (1986), Dalla Salda et al. (1992), Rapela et al. (1998), Davis et al. (2000), Gerbi et al. (2002), Ramos (2004), Thomas et al. (2012), González Menéndez et al. (2013) and Boedo et al. (2013).

The El Nihuil Dolerites record a geochemical and isotopic signature similar to that exposed along the western Precordillera belt (Boedo et al. 2013) as a subduction unrelated type at continental margin (Dilek and Furnes 2011). Figure 11 summarized the tectonic scenario during extensional and compressional phases.

It is noteworthy that the El Nihuil mafic rocks record two different tectonic settings: a Mesoproterozoic crustal fragment (represented by gabbros, amphibolites and tonalites) and Lower Paleozoic intrusive MORB-dolerite dykes, such as the two sections defined by Davis et al. (1999) for the mafic belt of western Precordillera.

7 Final Remarks

1. The undeformed porphyritic dolerites composed of sills and dykes are the predominating type rocks in the 'El Nihuil Mafic Unit.'
2. The country rocks for the dolerites are the high deformed gabbros, amphibolites, and tonalites interpreted as part of the Mesoproterozoic continental crust, exposed mainly at the 'Loma del Petiso shear zone' and Lomas Orientales along the northern sector of the 'El Nihuil Mafic Unit.'
3. The highly deformed mafic rocks and dolerite dykes are in unconformity with the Río Seco de los Castaños Fm as a Silurian-Devonian marine-deltaic system which preserved primary sedimentary structures.
4. The dolerites are geochemically characterized as tholeiite type rocks, and plot within the MORB field in tectonic discrimination diagrams. The trace and REE patterns are coherent with this origin.
5. Geochemical data from the El Nihuil Dolerites record a less evolved E-MORB-type signature than the mafic-ultramafic belt known in western Precordillera region.
6. The K–Ar (WR ages) indicate that the dolerite dykes are a unique Lower Paleozoic mafic event exposed within the entire SRB.
7. The juvenile depleted mantle origin is therefore confirmed by positive εNd values ranging from +4.27 to +12.42 at 450 Ma and Nd model ages (second

stage) from 0.51 to 0.80 Ga. The obtained $^{87}Sr/^{86}Sr$ ratios varying from 0.7032 to 0.7050 are in agreement with ocean ridge tholeiites.

8. The El Nihuil dolerite rocks (dykes and sills with chilled margins) formed a non-subduction related ophiolite within a margin facing a shallow ocean basin and could be interpreted as intruded into pre-Lower Silurian sedimentary units at marine and slope environments.
9. These dolerite rocks are interpreted as a shallow section of the dismembered 'Famatinian ophiolite belt' emplaced during the Upper Ordovician-Lower Silurian extensional event, within a thinned continental crust environment on the western side of the Cuyania terrane.

Acknowledgements This research was partially funded by CONICET (PIP 199) and by grants from the University of La Plata, Argentina. Many thanks to our colleagues Leandro Ortiz and Diego Licitra for their help during fieldworks and laboratory sample preparation. We appreciate the suggestions and guidance during laboratory work by Prof. Koji Kawashita (Brazil) and Prof. Ricardo Varela (CIG). We thank Gabriela Coelho dos Santos for her technical collaboration in petrographical descriptions.

References

Abre P, Cingolani C, Zimmermann U, Cairncross B (2009) Detrital chromian spinels from Upper Ordovician deposits in the Precordillera terrane, Argentine: a mafic crust input. J South America Earth Sci, 28:407–418 (Special Issue on Mafic and Ultramafic complexes in South America and the Caribbean)

Abre P, Cingolani CA, Manassero MJ (this volume) The Pavón Formation as the Upper Ordovician unit developed in a turbidite sand-rich ramp. San Rafael Block, Mendoza, Argentina. In: Cingolani CA (Ed.) The pre-Carboniferous evolution of the San Rafael Block, Argentina. Implications in the SW Gondwana margin, Chapter, 5. Springer

Alonso JI, Gallastegui J, García-Sansegundo J, Farias P, Rodríguez Fernández LR, Ramos VA (2008) Extensional tectonics and gravitational collapse in an Ordovician passive margin: the Western Argentine Precordillera. Gondwana Res 13:204–215

Arévalo Jr R, McDonough WF (2010) Chemical variations and regional diversity observed in MORB. Chem Geol 271:70–85

Boedo EL, Vujovich GI, Kay SM, Ariza JP, Pérez Luján SB (2013) The E-MORB like geochemical features of the Early Paleozoic mafic-ultramafic belt of the Cuyania terrane, western Argentina. J S Am Earth Sci 48:73–84

Borrello AV (1963) Elementos del magmatismo simaico inicial en la evolución de la secuencia geosinclinal de la Precordillera. Instituto Nac. Inv. Ciencias Naturales y Museo Argentino de Ciencias Naturales "B. Rivadavia". Revista, Serie Ciencias Geológicas 1:1–19. Buenos Aires

Borrello AV (1969) Los geosinclinales de la Argentina. Dirección Nacional de Geología y Minería, Anales, v.14:1–188. Buenos Aires

Cingolani CA, Llambías EJ, Ortiz L (2000) El magmatismo básico pre-Carbónico del Nihuil, Bloque de San Rafael, Provincia de Mendoza, Argentina. 9° Congreso Geológico Chileno, 2:717–721. Puerto Varas, Chile

Cingolani CA, Uriz NJ, Marques J, Pimentel M (2012) The Mesoproterozoic U–Pb (LA-ICP-MS) age of the Loma Alta gneissic rocks: Basement remnant of the San Rafael Block, Cuyania terrane, Argentina. VIII South American Symposium on Isotope Geology, Medellin, Colombia, 1p. abstracts book

Cingolani CA, Basei MAS, Varela R, Llambías EJ, Chemale Jr F., Abre P, Uriz NJ, Marques, JC (this volume) The Mesoproterozoic Basement at the San Rafael Block, Mendoza Province

(Argentina): geochemical and isotopic age constraints. In: Cingolani CA (ed) The pre-Carboniferous evolution of the San Rafael Block, Argentina. Implications in the SW Gondwana margin, Chapter, 2 Springer

Criado Roqué P, Ibáñez G (1979) Provincia sanrafaelino-pampeana. In: Turner JCM (ed) Simposio de Geología Regional Argentina, No 2, vol 1. Academia Nacional de Ciencias, Córdoba, pp 837–869

Dalla Salda LH, Cingolani CA, Varela R (1992) Early Paleozoic orogenic belt of the Andes in southeastern South America: result of Laurentia-Gondwana collision? Geology 20:617–620

Dalla Salda LH, López de Luchi MG, Cingolani CA (1998) Laurentia-Gondwana collision: the origin of the Famatinian-Appalachian Orogenic Belt (A review). In: Pankhurst RJ, Rapela CW (eds) The Proto-Andean Margin of Gondwana, vol 142. Geological Society, London, Special Publications, pp 219–234

Davicino RE, Sabalúa JC (1990) El Cuerpo Básico de El Nihuil, Dto. San Rafael, Pcia. de Mendoza, Rep. Argentina. In Congreso Geológico Argentino, No. 11, Actas I. San Juan, pp 43–47

Davis J, Roeske S, McClelland W, Snee L (1999) Closing an ocean between the Precordillera terrane and Chilenia; early Devonian ophiolite emplacement and deformation in the southwest Precordillera. In: Ramos VA, Keppie JD (eds) Laurentia-Gondwana connections before Pangea, vol 336. Geological Society of America, Special Publication, pp 115–138

Davis J, Roeske S, McClelland W, Kay SM (2000) Mafic and ultramafic crustal fragments of the southwestern Precordillera terrane and their bearing on tectonic models of the early Paleozoic in western Argentina. Geology 28(2):171–174

DePaolo DJ (1981) Neodymium isotopes in the Colorado Front Range and crust–mantle evolution in the Proterozoic. Nature 291:193–196

Dessanti RN (1956) Descripción geológica de la Hoja 27-C Cerro Diamante (Provincia de Mendoza). Dirección Nacional de Geología y Minería, Boletín, vol 85. Buenos Aires, pp 1–79

Dilek Y, Furnes H (2011) Ophiolite genesis and global tectonics: geochemical and tectonic fingerprinting of ancient oceanic lithosphere. Geol. Soc. Am. Bull. 123:387–411

Gale A, Dalton C, Langmuir CH, Su Y, Schilling JG (2013) The mean composition of ocean ridge basalts. Geochem. Geophys. Geosyst. 14:489–517

Gerbi C, Roeske SM, Davis JS (2002) Geology and structural history of the southwestern Precordillera margin, northern Mendoza province, Argentina. J S Am Earth Sci 14:821–835

González-Menéndez L, Gallastegui G, Cuesta A, Heredia N, Rubio-Ordoñez A (2013) Petrogénesis of Early Paleozoic basalts and gabros in the western Cuyania terrane: constraints on the tectonic setting of the southwestern Gondwana margin (Sierra del Tigre, Andean Argentine Precordillera). Gondwana Res 24(1):359–376

González Díaz EF (1981) Nuevos argumentos en favor del desdoblamiento de la denominada "Serie de la Horqueta", del Bloque de San Rafael, Provincia de Mendoza. In 8° Congreso Geológico Argentino, Actas 3:241–256. San Luis

Haller MJ, Ramos VA (1984). Las ofiolitas famatinianas (Eopaleozoico) de las Provincias de San Juan y Mendoza. 9º Congreso Geológico Argentino, Actas 3:66–83. S.C. Bariloche

Haller MJ, Ramos VA (1993). Las ofiolitas y otras rocas afines. In: Ramos, V.A. (Ed.) Geología y Recursos Naturales de Mendoza, Relatorio 12° Congreso Geológico Argentino, pp 31–39

Irvine TN, Baragar WRA (1971) A guide to the chemical classification of the common volcanic rocks. Can J Earth Sci 8:523–548

Le Maitre RW (1989) A Classification of Igneous Rocks and Glossary of Terms. In Blackwell. Oxford, 193 pp

Liew TC, Hoffmann AW (1988) Precambrian crustal components, plutonic associations, plate environments of Hercynian Fold Belt of Central Europe: indications from Nd and Sr isotopic study. Contrib Mineral Petrol, 98:129–138

Linares E, Parica C, Parica P (1987) Catálogo de edades radimétricas determinadas para la República Argentina (IV años 1979–1980 realizadas por INGEIS y sin publicar y V años 1981–1982 publicadas). Publicaciones Especiales, Asociación Geológica Argentina, Serie B (Didáctica y Complementaria) n. 15:1–49

Malhburg Kay S, Ramos VA, Kay RW (1984) Elementos mayoritarios y trazas de las vulcanitas ordovícicas de la Precordillera Occidental: basaltos de rift oceánico temprano (¿) próximos al margen continental. 9° Congreso Geológico Argentino, Actas 2:48–65. S.C. de Bariloche

Nuñez E (1976) Descripción geológica de la Hoja 28-C "Nihuil". Unpublished report, Provincia de Mendoza. Servicio Geológico Nacional. Buenos Aires

Padula E (1949) Descripción geológica de la Hoja 28-C "El Nihuil". Unpublished report, Provincia de Mendoza. YPF.

Pearce JA, Cann JR (1973) Tectonic setting of basic volcanic rocks determined using trace element analyses. Earth Planet Sci Lett 19:290–300

Ramos VA (1984) Patagonia: un continente paleozoico a la deriva? IX Congreso Geológico Argentino (San Carlos de Bariloche). Actas 2:311–325

Ramos VA, Jordan T, Allmendinger R, Kay S, Cortés J, Palma M (1984) Chilenia: un terreno alóctono en la evolución paleozoica de los Andes Centrales. 10° Congreso Geológico Argentino, Actas 2:84–106

Ramos VA, Jordan T, Allmendinger R, Mpodozis C, Kay S, Cortés J, Palma M (1986) Paleozoic terranes of the central Argentine-Chilean Andes. Tectonics 5:855–888

Ramos VA, Dallmeyer RD, Vujovich G (1999) Time constraints on the Early Palaeozoic docking of the Precordillera, central Argentina. In Pankhurst RJ, Rapela CW (eds) The Proto-Andean Margin of Gondwana, vol 142. Geological Society, Special Publications. London, pp 143–158

Ramos VA, Escayola M, Mutti DI, Vujovich GI (2000) Proterozoic-early Paleozoic ophiolites of the Andean basement of southern South America. In: Dilek Y, Moores EM, Elthon D, Nicolas A (eds.) Ophiolites and Oceanic crust: New insights from Field Studies and the Ocean Drilling Program: Boulder, Colorado, vol 349. Geological Society of America, Special Paper, pp 331–349

Ramos VA (2004) Cuyania, an exotic block to Gondwana: Review of a historical success and the present problems. Gondwana Res 7:1009–1026

Rapela CW, Pankhurst RJ, Casquet C, Baldo E, Saavedra J, Galindo C (1998) Early evolution of the Proto-Andean margin of South America. Geology 26:707–710

Sepúlveda E (1999) Descripción geológica preliminar de la Hoja Embalse El Nihuil, provincia de Mendoza, escala 1:250.000. SEGEMAR, Boletín, vol 268. Buenos Aires, pp 84

Sepúlveda E, Carpio FW, Regairaz MC, Zárate M, Zanettini JCM (2007) Hoja Geológica 3569-II (San Rafael, Provincia de Mendoza). Servicio Geológico Minero Argentino, Boletín 321, Buenos Aires, 59 pp

Taylor SR, McLennan SM (1985) The continental crust. Its composition and evolution. Blackwell, London 312 pp

Thomas WA, Tucker RD, Astini RA, Denison RE (2012) Ages of pre-rift basement and synrift rocks along the conjugate rift and transform margins of the Argentine Precordillera and Laurentia. Geosphere 8(6):1366–1383

Winchester JA, Floyd PA (1976) Geochemical magma type discrimination, application to altered and metamorphosed basic igneous rocks. Earth Planet Sci Lett 28(3):325–343

Winchester JA, Floyd PA (1977) Geochemical discrimination of different magma series and their differentiation products using immobile elements. Chem Geol, 20:325–343

Wood DA, Joron JL, Treuil M (1979) A reappraisal of the use of trace elements to classify and discriminate between magma series erupted in different tectonic settings. Earth Planet Sci Lett 45(2):326–336

Wichmann R (1928) Reconocimiento geológico de la región de El Nihuil, especialmente relacionado con el proyectado dique de embalse del Río Atuel. Dirección Nacional de Minería (unpublished report), Buenos Aires